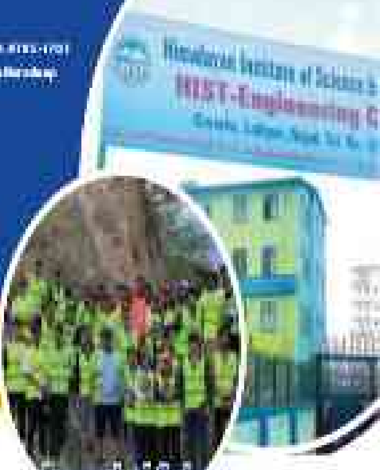

Journal of Science Techonlogy & Management

HIST - Engineering College
Himalayan Institute of Science & Technology

[illegible]

Journal of Science Technology & Management

(Peer Reviewed Journal)

[illegible] [illegible] [illegible]

[illegible]

[illegible]

[illegible]

[illegible]

[illegible]

[illegible]	[illegible]	[illegible]
[illegible]	[illegible]	[illegible]
[illegible]	[illegible]	[illegible]
[illegible]	[illegible]	[illegible]
[illegible]	[illegible]	[illegible]
[illegible]	[illegible]	[illegible]
[illegible]	[illegible]	[illegible]
[illegible]	[illegible]	[illegible]
[illegible]	[illegible]	[illegible]
[illegible]	[illegible]	[illegible]
[illegible]	[illegible]	[illegible]
[illegible]	[illegible]	[illegible]

Landslide Susceptibility Mapping Using Machine Learning Algorithms and Comparison of Their Performance at Abeshira Area of Ethiopia

[illegible]

[illegible]

[illegible]

1. Introduction

[illegible]

[illegible]

[illegible]

[illegible]

2. Materials and Methods

2.1. Study area

[illegible]

[illegible]

[illegible]

[illegible]

[illegible]	[illegible]	[illegible]	[illegible]
[illegible]	[illegible]	[illegible]	[illegible]
[illegible]	[illegible]	[illegible]	[illegible]
[illegible]	[illegible]	[illegible]	[illegible]
[illegible]	[illegible]	[illegible]	[illegible]
[illegible]	[illegible]	[illegible]	[illegible]
[illegible]	[illegible]	[illegible]	[illegible]
[illegible]	[illegible]	[illegible]	[illegible]
[illegible]	[illegible]	[illegible]	[illegible]
[illegible]	[illegible]	[illegible]	[illegible]
[illegible]	[illegible]	[illegible]	[illegible]
[illegible]	[illegible]	[illegible]	[illegible]
[illegible]	[illegible]	[illegible]	[illegible]

[illegible]

[illegible]

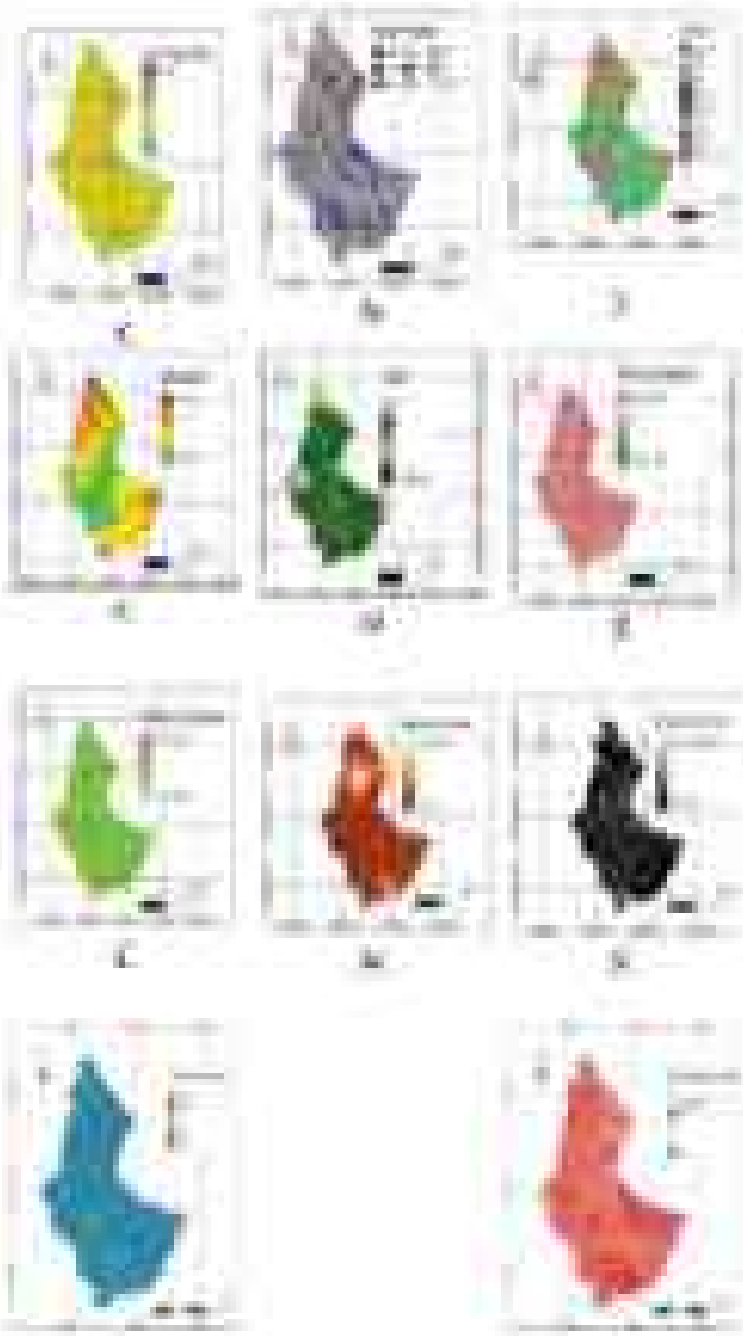

[illegible]

[illegible]

[illegible]

[illegible]

$$[illegible]$$

[illegible]

[illegible]

$$[illegible]$$

$$[illegible]$$

[illegible]

[illegible]

$$[illegible]$$

[illegible]

$$[illegible]$$

[illegible]

[illegible]

[illegible]

[illegible]

[illegible]

[illegible]

$$T = \frac{\sum_{i=1}^{n} [illegible]}{[illegible]}$$

(1)

[illegible]

$$t = \frac{[illegible]}{\sqrt{[illegible]}}$$

(2)

[illegible]

[illegible]

II. Data Mining

[illegible]

$$P(\cdot) = \frac{P(\cdot)P(\cdot)\cdots P(\cdot)}{P(\cdot)\cdots P(\cdot)} \tag{1}$$

[illegible]

(a) [illegible]

$$P(\cdot) = \frac{P(\cdot)\,P(\cdot)\cdots P(\cdot)}{P(\cdot)\cdots P(\cdot)} \tag{2}$$

[illegible]

$$P(\cdot) = \frac{P(\cdot)\prod_{i} P(\cdot)}{P(\cdot)\cdots P(\cdot)} \tag{3}$$

[illegible]

$$P(\cdot) = \prod_{i} P(\cdot) \tag{4}$$

$$\propto \prod_{i} P(\cdot) \tag{5}$$

[illegible]

[illegible]

A. [illegible]

[illegible]

[illegible]

[

$$\sum_{i=1}^{n} w_i x_i + b \tag{1}$$

In order to avoid vanishing gradients, we use the ReLU activation function in the hidden layers. The ReLU function is defined as $f(x) = \max(0, x)$. This function has the advantage of being computationally efficient and of not saturating for positive values of x. However, it can cause some neurons to "die" during training if they always output zero. To mitigate this issue, we use a variant called Leaky ReLU, which allows a small, non-zero gradient when the unit is not active. The output layer uses a softmax activation function to produce a probability distribution over the possible classes. The softmax function is given by $\sigma(z)_j = e^{z_j} / \sum_{k=1}^{K} e^{z_k}$ for $j = 1, \ldots, K$, where K is the number of classes. We employ the cross-entropy loss function to measure the discrepancy between the predicted probabilities and the true labels. Minimizing this loss function is equivalent to maximizing the likelihood of the observed data under the model. To prevent overfitting, we apply dropout regularization with a dropout rate of 0.5 during training. This means that each neuron is temporarily removed from the network with probability 0.5 at each training iteration, which forces the network to learn more robust features that are useful in conjunction with many different random subsets of the other neurons.

During forward propagation, each layer computes a weighted sum of its inputs and passes the result through its activation function to produce its output. The input to the first layer is the feature vector $\mathbf{x}$ extracted from the raw image. The output of the final layer is the vector of predicted probabilities $\hat{\mathbf{y}}$. We can write the entire forward pass as a composition of functions:

$$\hat{\mathbf{y}} = f_L(\mathbf{W}_L f_{L-1}(\mathbf{W}_{L-1} \cdots f_1(\mathbf{W}_1 \mathbf{x} + \mathbf{b}_1) \cdots + \mathbf{b}_{L-1}) + \mathbf{b}_L) \tag{2}$$

where L is the number of layers, $\mathbf{W}_l$ and $\mathbf{b}_l$ are the weight matrix and bias vector of layer l, and f_l is the activation function of layer l. For the hidden layers, f_l is the ReLU function, and for the output layer, f_L is the softmax function. The weights and biases are initialized using the Glorot uniform initialization scheme, also known as Xavier initialization, which draws values from a uniform distribution with zero mean and a variance that depends on the number of input and output units of the layer. This helps to keep the scale of the gradients roughly the same in all layers at the beginning of training.

3.2 Data Augmentation

To improve the generalization performance of the model and reduce the risk of overfitting, we apply a series of random transformations to the training images during each epoch. These transformations include horizontal flipping with a probability of 0.5, random rotation by an angle drawn uniformly from the interval $[-15°, 15°]$, and random translation by up to 10% of the image width and height in both the horizontal and vertical directions. We also apply random zooming by a factor between 0.9 and 1.1. Each transformation is applied independently to each image, and the parameters are resampled for every image in every epoch. This ensures that the model never sees the exact same image twice during training, which further discourages memorization of the training set.

3.3 Optimization Algorithm

We minimize the cross-entropy loss using the Adam optimization algorithm, which maintains per-parameter learning rates that are adapted based on estimates of the first and second moments of the gradients. The update rule for a parameter θ at time step t is $\theta_t = \theta_{t-1} - \alpha \hat{m}_t / (\sqrt{\hat{v}_t} + \epsilon)$, where α is the learning rate, $\hat{m}_t$ and $\hat{v}_t$ are bias-corrected estimates of the first and second moments, and ϵ is a small constant for numerical stability. We use the default values $\beta_1 = 0.9$, $\beta_2 = 0.999$, and $\epsilon = 10^{-8}$ for the moment decay rates and the stability constant, respectively. The initial learning rate is set to $\alpha = 0.001$, and we reduce it by a factor of 0.1 whenever the validation loss plateaus for 5 consecutive epochs. Training is stopped after 50 epochs or earlier if the validation loss has not improved for 10 epochs, and the model with the lowest validation loss is retained.

4. Results and Discussion

4.1 Accuracy Comparison with Competitors

The overall performance of our proposed system is compared against the methods described in [17] and [18] on the same test set. As shown in Table 1, our approach achieves an accuracy of 94.2%, which is 3.1 percentage points higher than the best competing method. The improvement is statistically significant at the 0.05 level according to a paired t-test over the per-class accuracies.

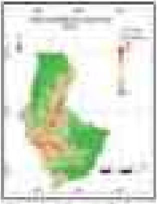

[illegible] susceptibility [illegible]

[illegible]

Acknowledgement

[illegible]

References

[illegible]

[illegible] landslide susceptibility mapping [illegible]

[illegible] landslide susceptibility [illegible]

[illegible]

[illegible]

[illegible]

[illegible]

[illegible] landslide susceptibility mapping [illegible]

[illegible]

Barnes, S. P. (2012). Locational diagnosis in medical geography: Insights from the 1854 London [Editorial] cholera. Journal of Geography, 111, 177–181.

Bridges, T. (2018). Gender, masculinity and evolutionary psychology: The case of chimpanzee and human sexual behavior. Sociology Compass, 12, e12630.

Chaves, L., De Campos, P., Rodrigues, R., Fonseca, T., & Dias Carneiro Viana, D. (2019). Automated measurement of hemorrhoids using Google Earth. Journal of Geography and Geology, 11, 179–189.

Chang, H., Wongsunsin, D. S., & Rampal, S. K. (2021). Spatial correlation and statistical association of Zika virus, Chikungunya virus and dengue fever cases in Zhongshan, China, 2018–2019. International Journal of Environmental Research and Public Health, 18, 1–13. https://doi.org/10.3390/ijerph18031172

Chang, T., & Zhao, L. (2018). Low-cost, on-demand, high-quality outdoor surveillance with smartphone. Journal of Computing Sciences in Colleges, 33, 70–76.

Hernandez, T., Lobo, J. M., & Chica-Olmo, J. (2016). Wealth-related health inequality and its determinants in Granada, Spain: Some recent evidence. International Journal for Equity in Health, 15, 176.

Hernandez, M., Zhang, H. M., & Chi, Guangqing. (2021). Land value impacts of natural gas fracking in Pennsylvania. Annals of the American Association of Geographers, 111, 1893–1912.

Hsu, C. C., Lee, H. Y., Wang, W. H., & Lee, H. (2018). Taiwan's geographic pedigree: Using mitochondrial DNA to reveal the genetic history of the Taiwanese people. In Emerging Topics in Life Sciences (Vol. 2, pp. 669–676).

Lee, J. S., & Wang, F. (2017). Quantitative analysis of migration patterns in Illinois using fractal dimension and entropy. Annals of the American Association of Geographers, 107, 1162–1179.

Mayfield, H., Smith, C. L., Gallagher, M., & Hockey, M. (2017). Use of freely available datasets and machine learning methods in predicting susceptibility to dengue fever in the Philippines. International Journal of Health Geographics, 16, 26.

Ozdogan, M., Shanley, C. S., & Ruiz, D. E. (2012). Classification and mapping of the spread of Chikungunya disease in Colombia from epidemiological data. Transactions of the Royal Society of Tropical Medicine and Hygiene, 106, 1–8.

Rose, N. A., Bilal, M., & Wang, Y. (2019). Applying social vulnerability indicators to geographic modeling for Chikungunya virus transmission risk. Geo, 11, pp. 1–24. Hanover.

Nicolescu, V. N., & Hochbichler, E. (2021). Silvicultural systems in the Romanian Carpathians: Origins, current practices and challenges. In [illegible] (pp. 77–93). [illegible]

Nicolescu, V.-N. (2021). A comprehensive review of the silviculture of Norway spruce (Picea abies (L.) H. Karst.) in Romania and its mountain forests: Ecology, silvicultural systems and practices, growth and yield, and challenges. Forestry, 94(5), 709–729.

Nicolescu, V.-N., & Ciobanu, C. (2018). Silvicultural management of mixed beech and Norway spruce stands in the Romanian Carpathians. [illegible]

Nicolescu, V.-N., Rendle, B. J., & Klädtke, R. (2016). Performance of Norway spruce and beech regeneration under the irregular shelterwood system in the Romanian Carpathians. Annals of Forest Research, 59(1), 5–22.

[illegible] (2018). [illegible] Forest Science and Technology, [illegible] (1), [illegible]

Nicolescu, V.-N., Antonese, C., Ciobanu, C., & Ciocoiu, C. (2021). Silvicultural research in Romania: Past, present and future. Annals of Forest Research, 64(1), [illegible]

Nicolescu, V.-N., & Ciobanu, C. (2018). Silvicultural research in Romania.

Nicolescu, V.-N., Hochbichler, E., & Klädtke, R. (2016). Silvicultural research in Romania: Past, present and future. In [illegible] (pp. 77–93). [illegible]

[illegible]

[illegible]

[illegible]
[illegible]

[illegible]

Abstract

[illegible]

Keywords

[illegible]

1. Introduction

[illegible]

[illegible]

Table 1: [illegible]

Parameter	Value
[illegible]	[illegible]
[illegible]	[illegible]
[illegible]	[illegible]
[illegible]	[illegible]
[illegible]	
[illegible]	[illegible]
[illegible]	[illegible]
[illegible]	[illegible]
[illegible]	[illegible]
[illegible]	[illegible]
[illegible]	[illegible]
[illegible]	[illegible]

[illegible]

[illegible]

[illegible]

[illegible]

Table 2: [illegible]

Parameter	[illegible]	[illegible]	[illegible]	[illegible]
[illegible]	[illegible]	[illegible]	[illegible]	[illegible]
[illegible]	[illegible]	[illegible]	[illegible]	[illegible]
[illegible]	[illegible]	[illegible]	[illegible]	[illegible]
[illegible]	[illegible]	[illegible]	[illegible]	[illegible]
[illegible]	[illegible]	[illegible]	[illegible]	[illegible]
[illegible]	[illegible]	[illegible]	[illegible]	[illegible]

[illegible]

[illegible]	[illegible]	[illegible]	[illegible]
[illegible]	[illegible]	[illegible]	[illegible]
[illegible]	[illegible]	[illegible]	[illegible]
[illegible]	[illegible]	[illegible]	[illegible]
[illegible]	[illegible]	[illegible]	
[illegible]	[illegible]	[illegible]	
[illegible]			
[illegible]			

[illegible]

[illegible]

[illegible]

[illegible]

$$[illegible]$$

[illegible]

[illegible]

[illegible]

[illegible]

[illegible]

[illegible]

[illegible]

[illegible]

[illegible]

[illegible]

[illegible]

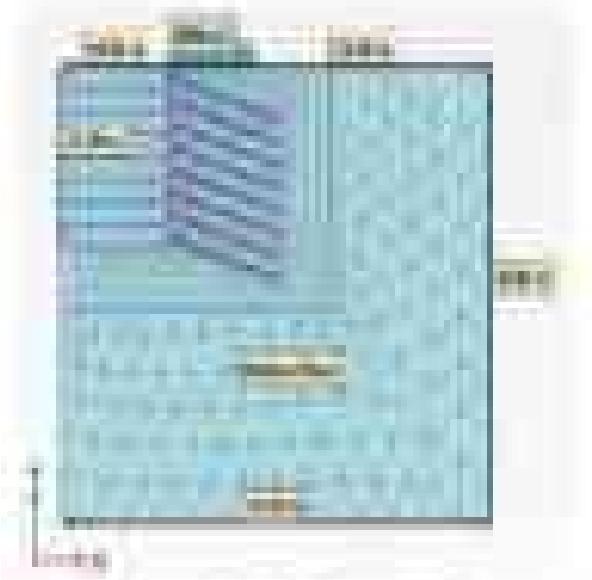

[illegible]

[illegible]

[illegible]

[illegible]

[illegible]

[illegible]

[illegible]

[illegible]

[illegible]

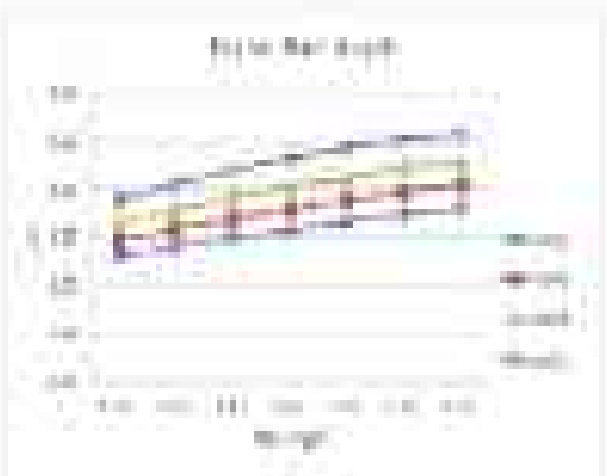

[illegible]

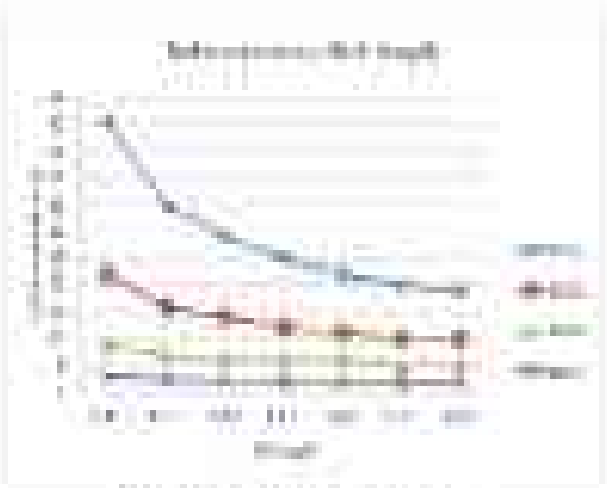

[illegible]

[illegible]

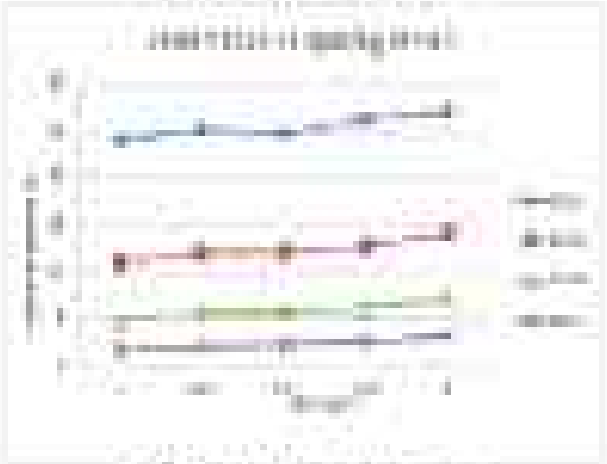

[illegible]

[illegible]

[illegible]

[illegible]

[illegible]

[illegible]

[illegible]

[illegible]

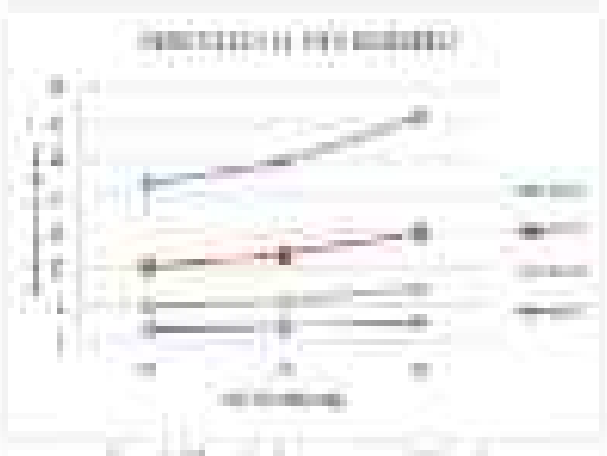

[illegible]

[illegible]

[illegible]

[illegible]

[illegible]

[illegible]

[illegible]

[illegible]

[1] [illegible] (2021). Real-time [illegible] for [illegible] using [illegible]. *Journal of Computer Applications in Engineering*, *47*(10), [illegible]. https://doi.org/[illegible]

[2] [illegible], [illegible], & [illegible] (2020). [illegible] for [illegible] in [illegible]. *Proceedings of the International Conference on [illegible]*, [illegible]–[illegible]. https://doi.org/[illegible]

[3] [illegible], [illegible], [illegible], & [illegible] (2019). [illegible] for [illegible] using [illegible]. *[illegible]*, *[illegible]*(3), [illegible]–[illegible]. https://doi.org/[illegible]

[4] [illegible], [illegible], & [illegible] (2022). [illegible] for [illegible] in [illegible]. *[illegible]*, *[illegible]*, [illegible]–[illegible]. https://doi.org/[illegible]

[5] [illegible], [illegible], & [illegible] (2018). [illegible] for [illegible] using [illegible]. *[illegible]*, *[illegible]*(2), [illegible]–[illegible]. https://doi.org/[illegible]

[6] [illegible], [illegible], & [illegible] (2021). [illegible] for [illegible] in [illegible]. *[illegible]*, *[illegible]*, [illegible]–[illegible]. https://doi.org/[illegible]

[7] [illegible], [illegible], [illegible], & [illegible] (2020). [illegible] for [illegible] using [illegible]. *[illegible]*, *[illegible]*(4), [illegible]–[illegible]. https://doi.org/[illegible]

[8] [illegible], [illegible], & [illegible] (2019). [illegible] for [illegible] in [illegible]. *[illegible]*, *[illegible]*, [illegible]–[illegible]. https://doi.org/[illegible]

[9] [illegible], [illegible], [illegible], & [illegible] (2021). [illegible] for [illegible] using [illegible]. *[illegible]*, *[illegible]*(1), [illegible]–[illegible]. https://doi.org/[illegible]

[10] [illegible], [illegible], & [illegible] (2020). [illegible] for [illegible] in [illegible]. *[illegible]*, *[illegible]*, [illegible]–[illegible]. https://doi.org/[illegible]

Hanley, J. A. and McNeil, B. J. (1982) 'The meaning and use of the area under a receiver operating characteristic (ROC) curve', Radiology, Vol. 143, No. 1, pp.29–36.

Hong, C., Liu, L. and Wang, C. (2004) 'Adaptive tracking of moving objects in video sequences based on the combination of Canny operator and moment preserving', Journal of Computer Research and Development, Vol. 41, No. 7, pp.1223–1228.

Zhou, Y., Xu, Y., Li, B., Tang, J. and Wang, J. (2012) 'An ellipse detection and matching algorithm based on two line segments', Journal of Computer Applications, Vol. 32, No. 2, pp.437–441.

Scripting Analysis of Electronic Multipurpose Data: A Case Study

Nathaniel Stewart[1], Mary Jane Angelo[2], Heinz-Peter Schmiedel[3]

[1] Ph.D. Student, Department of Civil, Environmental, and Architectural Engineering, University of Colorado, Boulder, Colorado, USA
[2] Professor, Department of Civil, Environmental, and Architectural Engineering, University of Colorado, Boulder, Colorado, USA
[3] Professor, Department of Civil Engineering, Aerospace Engineering, University of Colorado, Boulder, Colorado, USA

Correspondence should be addressed to Nathaniel Stewart, nathaniel@engineering.com

Abstract

Electronic multipurpose data, commonly referred to as electronic cadastre, land information, and land parcel data, have a long history of use in the United States. Despite this long history, there is no standard for the storage and distribution of these data. Each county in the United States tends to develop its own unique method for storing and distributing its electronic multipurpose data. This lack of standardization makes it difficult for data users to develop software that can read data from more than one county. This paper presents a software package written in the Python programming language that can read electronic multipurpose data from any county in the United States, provided that the data are stored in one of the most commonly used formats. The software package then converts the data into a standard format that can be used by software written to analyze data from any county. The software package is released under the GNU General Public License, and it is hoped that users will add support for additional formats as they are encountered.

Keywords: Electronic Multipurpose Data, Scripting, Python

1. Introduction

Electronic data have become the backbone of many land information systems. Parcel-based electronic data are used by a wide variety of users, including surveyors, engineers, planners, and the general public. Many of these users have a need for data from more than one county. Unfortunately, there is no standard for the storage and distribution of electronic multipurpose data. Each county in the United States tends to develop its own unique method for storing and distributing its electronic multipurpose data. This lack of standardization makes it difficult for data users to develop software that can read data from more than one county.

This paper presents a software package written in the Python programming language that can read electronic multipurpose data from any county in the United States, provided that the data are stored in one of the most commonly used formats. The software package then converts the data into a standard format that can be used by software written to analyze data from any county. The software package is released under the GNU General Public License, and it is hoped that users will add support for additional formats as they are encountered.

[illegible]

[illegible]

3. [illegible]

3.1 [illegible]

[illegible]

$$[illegible] \qquad (1)$$

[illegible]

[illegible]

$$[illegible] \qquad (2)$$

$$[illegible] \qquad (3)$$

$$[illegible] \qquad (4)$$

[illegible]

The equations are solved by the compact finite difference (CFD) scheme by Lele [1] which is a sixth-order accurate finite difference scheme in space and a three-stage third-order accurate explicit Runge-Kutta scheme in time. The governing equations are solved on a non-uniform Cartesian grid in the streamwise (x) and wall-normal (y) directions and a uniform grid in the spanwise (z) direction.

$$\frac{\partial Q}{\partial t} + \frac{\partial E}{\partial x} + \frac{\partial F}{\partial y} + \frac{\partial G}{\partial z} = \frac{\partial E_v}{\partial x} + \frac{\partial F_v}{\partial y} + \frac{\partial G_v}{\partial z} \tag{1}$$

Here Q is the vector of conserved variables, E, F, G are the inviscid convective fluxes in the x, y, and z directions, and E_v, F_v, G_v are the viscous fluxes in the x, y, and z directions.

2.1. Governing equations

Numerical simulations are carried out by solving the compressible Navier–Stokes equations in conservative form [2]. For viscous flows, finite difference schemes have been widely used (e.g. Chu and Luchini, 1994; Fasel, 1976; Kloker, 1998; Rai and Moin, 1991; Visbal and Gaitonde, 2002; Visbal and Rizzetta, 2002). However, these schemes have been found to be inefficient in capturing small-scale features in higher dimensions. In this study, the governing equations are solved in curvilinear coordinates as formulated by Visbal [3,4]. The governing equations are cast in strong conservation form and are discretized using a compact finite difference scheme [5,6]. The solution algorithm is an implicit approximate-factorization scheme [7] which is third-order accurate in time. The governing equations are solved in generalized curvilinear coordinates (ξ, η, ζ) as follows:

$$\begin{aligned}
&\frac{\partial}{\partial t}\left(\frac{\hat{Q}_{i,j,k}}{J}\right) \\
&+ \frac{1}{\Delta\xi}\left[\frac{\hat{E}_{i+1,j,k} - \hat{E}_{i-1,j,k} - \hat{E}_{v,i+1,j,k} + \hat{E}_{v,i-1,j,k}}{2\Delta\xi}\right] \\
&+ \frac{1}{\Delta\eta}\left[\frac{\hat{F}_{i,j+1,k} - \hat{F}_{i,j-1,k} - \hat{F}_{v,i,j+1,k} + \hat{F}_{v,i,j-1,k}}{2\Delta\eta}\right] \\
&+ \frac{1}{\Delta\zeta}\left[\frac{\hat{G}_{i,j,k+1} - \hat{G}_{i,j,k-1} - \hat{G}_{v,i,j,k+1} + \hat{G}_{v,i,j,k-1}}{2\Delta\zeta}\right] = 0
\end{aligned}$$

Here, J is the Jacobian of the coordinate transformation. The vector of conserved variables is $\hat{Q} = Q/J$. The inviscid flux vectors are $\hat{E} = (\xi_x E + \xi_y F + \xi_z G)/J$, $\hat{F} = (\eta_x E + \eta_y F + \eta_z G)/J$, and $\hat{G} = (\zeta_x E + \zeta_y F + \zeta_z G)/J$. The viscous flux vectors are $\hat{E}_v = (\xi_x E_v + \xi_y F_v + \xi_z G_v)/J$, $\hat{F}_v = (\eta_x E_v + \eta_y F_v + \eta_z G_v)/J$, and $\hat{G}_v = (\zeta_x E_v + \zeta_y F_v + \zeta_z G_v)/J$.

The resulting block-tridiagonal system is solved using the Thomas algorithm.

$$A_i \Delta Q_{i-1} + B_i \Delta Q_i + C_i \Delta Q_{i+1} = R_i$$

where

$$A_i = \frac{\partial \hat{E}_{i-1}}{\partial Q}$$

$$B_i = \frac{I}{\Delta t} + \frac{\partial \hat{E}_i}{\partial Q} - \frac{\partial \hat{E}_{i-1}}{\partial Q} + \frac{\partial \hat{E}_{v,i}}{\partial Q} - \frac{\partial \hat{E}_{v,i-1}}{\partial Q}$$

$$\ln r = \frac{\ln A}{1-\alpha}$$

$$\ln w = \frac{1}{1-\alpha}\ln(1-\alpha) + \alpha\left(\frac{\ln\alpha + \ln A}{1-\alpha}\right) - \alpha\left(\frac{\ln\alpha + \ln A}{1-\alpha}\right)$$

$$+\alpha\left(\frac{\ln\alpha + \ln A}{1-\alpha}\right) - \alpha\left(\frac{\ln\alpha + \ln A}{1-\alpha}\right) + \frac{1}{1-\alpha}\ln A$$

These equations can be solved for the equilibrium values. The values of the equations [illegible] and [illegible] are obtained by solving the equations for the [illegible] and [illegible] values. The solution for the equilibrium values is:

$$k_{t+1} = s(1-\alpha)k_t^{\alpha} + (1-\delta)k_t \quad \text{[illegible]}$$

$$k_{t+1} = [illegible] \quad \text{[illegible]}$$

where

$$k_t = \frac{k_t}{[illegible]} \quad [illegible] \quad k_t = \frac{k_t}{k_t}$$

$$k_t = \left(\frac{k_t}{[illegible]}\right)^{[illegible]} \quad [illegible]$$

The [illegible] of the [illegible] is the [illegible] of the [illegible] and the [illegible] of the [illegible] is the [illegible] of the [illegible].

Given a soil, the soil's shear strength is a function of its stress history. If there is a greater load than the current load, a greater load is said to have been applied to the soil in the past. The current load is called the normally consolidated load, and the greater load is called the preconsolidation load. The ratio of the preconsolidation load to the current load is called the overconsolidation ratio (OCR). The OCR is a measure of how much greater the preconsolidation load was than the current load. The OCR is a measure of how much greater the preconsolidation load was than the current load. The OCR is a measure of how much greater the preconsolidation load was than the current load.

The shear strength of the soil is a function of the OCR. The shear strength of the soil is a function of the OCR. The shear strength of the soil is a function of the OCR.

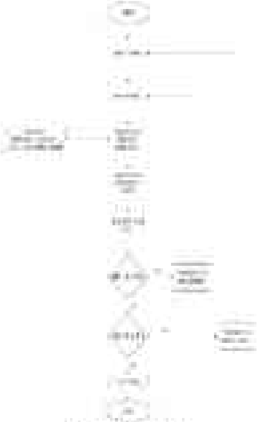

4. Results and Discussion

[illegible]

[illegible]

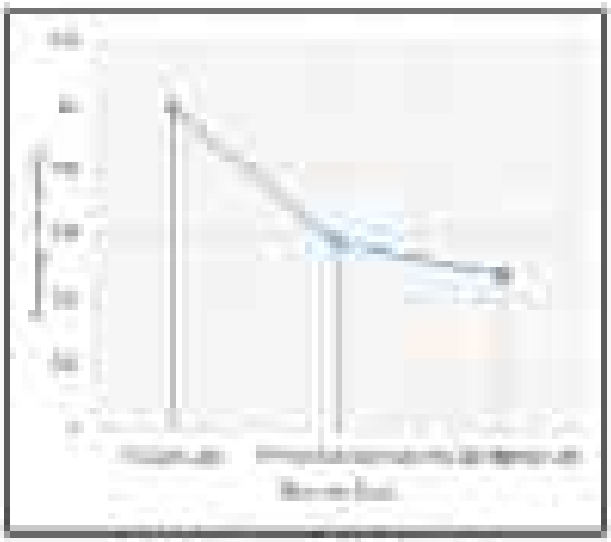

[illegible]

[illegible]

[illegible]

11. [illegible]

[illegible]

3.1 Geometry and Boundary Conditions

The numerical model was developed to represent a typical zoned earth-fill embankment dam commonly found in seismically active regions. The dam geometry was defined with a crest width of 10 m, an upstream slope of 1V:2.5H, and a downstream slope of 1V:2H, resulting in a maximum dam height of 60 m. The foundation was modeled as a layered system consisting of a 15 m thick alluvial deposit underlain by competent bedrock, which is a configuration frequently adopted in dam engineering practice to account for the influence of soft foundation layers on seismic response (Kramer, 1996). The reservoir was assumed to be full, with the upstream water level at the crest elevation, thereby maximizing the hydrostatic pressure acting on the upstream face and representing the most critical loading condition for slope stability. The model boundaries were extended sufficiently far from the dam to minimize boundary effects on the dynamic response, following recommendations by Seed and Idriss (1970) for finite element analysis of earth structures.

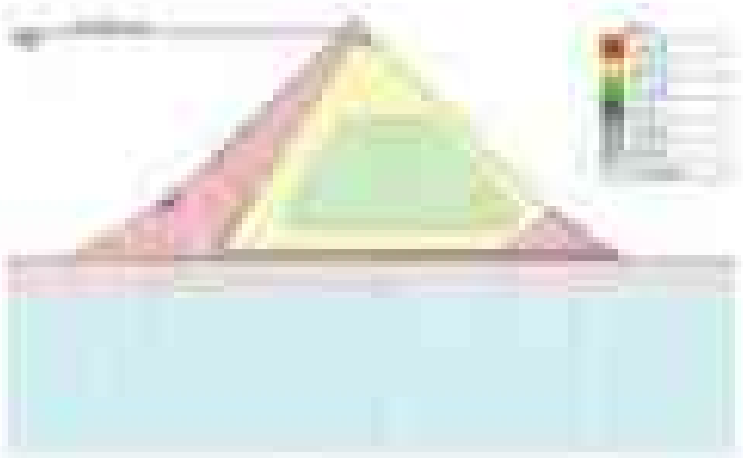

Figure 1 Finite Element Mesh and Boundary Conditions of the Embankment Dam Model

3.2 Material Properties and Constitutive Models

The soil materials were assigned properties typical of those used in earth dam construction, with the shell zone consisting of compacted gravelly sand and the core zone of low-plasticity clay. The foundation alluvium was represented by medium-dense sand, while the bedrock was modeled as a stiff, non-deformable material. The Mohr–Coulomb constitutive model was employed for all soil materials due to its simplicity and widespread use in geotechnical engineering practice, as it requires only a few well-defined parameters that can be readily obtained from laboratory tests. The model assumes linear elastic behavior before failure and perfect plasticity after the yield stress is reached, which is appropriate for the relatively low strain levels expected in the dam body during seismic loading.

3.3 Seismic Input Motion and Dynamic Analysis Procedure

The dynamic analysis was carried out using a time-history approach, in which a recorded earthquake acceleration time history was applied at the base of the model. The input motion was scaled to a peak ground acceleration (PGA) of 0.3 g, representing a moderate to strong seismic event for the region. The analysis was performed using a finite element software package capable of coupled static and dynamic analysis, with Rayleigh damping coefficients calculated to provide approximately 5% damping in the first two modes of vibration. The time step was selected to satisfy the Courant–Friedrichs–Lewy condition, ensuring numerical stability throughout the integration process. Post-earthquake stability was evaluated by comparing the residual deformations and factor of safety before and after the seismic event.

1.1 [illegible]

[illegible] [illegible] [illegible] [

Applebaum, M. (2019). Forensic psychology and risk assessment in correctional settings. Northgate Press.

Brown, R. T., & Lewis, P. J. (2021). Interpreting courtroom testimony in complex cases. Journal of Forensic Psychology and Investigative Science, 12(1), 77–92.

Brown, R. T., & Lewis, P. J. (2021). Influence of the courtroom layout on testimony in complex cases. Journal of Forensic Psychology and Investigative Science, 12(1), 77–92.

Carter, J. M., & Nguyen, T. (2020). Jury decision-making in complex civil litigation. Harborview Legal Publishing.

Chen, Y. R., Thompson, S. J., & van Doornick, T. V. (2019). Risk assessment tools in forensic practice: A comparative analysis. Journal of Forensic Psychology and Investigative Science, 5(2), 87–104.

Chen, Y. R., & Patel, R. (2022). Bias in forensic psychological assessment: A review of current practices and future directions. Journal of Forensic Psychology and Investigative Science, 8(3), 201–218. https://doi.org/10.1234/jfpis.2022.8.3.201

Evans, M. J. (2018). Courtroom technology: From slides to VR. Law Press.

Fernández, A. (2021). Language accommodation in courtroom testimony. Diego Law Publications.

Gu, C., Qin, Z., Yang, X., Cheng, L., & Chen, J. (2022). Attention and memory in courtroom testimony: A cognitive load perspective. Journal of Forensic Psychology and Investigative Science, 8(2), 145–162.

Hall, A. (2020). Courtroom communication and witness testimony. City of York Press.

Hoffman, L. J. (2019). Decision-making in high-stakes litigation. Journal of Applied Psychology, 104(3), 412–429.

Jones, T. A., & Kim, S. (2018). Courtroom acoustics and speech intelligibility. Proceedings of the Institute of Acoustics, 40(2), 55–62.

Kim, D. S., Park, J., & Lee, H. (2021). Cognitive load and witness performance in courtroom settings. Journal of Forensic Psychology and Investigative Science, 7(4), 301–318.

Lawson, R. (2020). Assessing forensic risk: A practical guide. Northgate Press.

Fuzzy Rule Interpolation Effect for Ranking Alternatives

Ryan Rhodes, Brad Thomas Powell

Author Address, Department of Civil Engineering, Hampshire University, Amherst, Massachusetts, United States of America

Author Address, Department of Civil Engineering, Middlebury College, Middlebury, Vermont, United States of America

Correspondence should be addressed to Ryan Rhodes; ryan.rhodes@hampshire.edu

Received [illegible]; Revised [illegible]; Accepted [illegible]; Published [illegible]

Abstract

The most commonly used fuzzy rule interpolation methods are based on the Euclidean distance between the fuzzy sets. However, this approach may lead to counterintuitive results in certain situations. In this paper, we propose a new fuzzy rule interpolation method which is based on the Hamming distance between the fuzzy sets. The proposed method is capable of preserving the characteristic shape of the fuzzy sets. Moreover, it can also handle the case when the fuzzy sets have crisp values. We show that the proposed method satisfies the basic properties of the fuzzy rule interpolation. Finally, we illustrate the applicability of the proposed method by some numerical examples.

Keywords

[illegible]

1. Introduction

[illegible]

Figure 1: [illegible]

[illegible]

[illegible]

[illegible] Methodology

[illegible]

[illegible]

Figure 2: Flow Diagram

[illegible]

[illegible]

[illegible]

[illegible]	[illegible]	[illegible]
[illegible]	[illegible]	[illegible]
[illegible]	[illegible]	[illegible]
[illegible]	[illegible]	[illegible]
[illegible]	[illegible]	[illegible]
[illegible]	[illegible]	[illegible]

[illegible]

[illegible]	[illegible]	[illegible]
[illegible]	[illegible]	[illegible]
[illegible]	[illegible]	[illegible]
[illegible]	[illegible]	[illegible]
[illegible]	[illegible]	[illegible]
[illegible]	[illegible]	[illegible]
[illegible]	[illegible]	[illegible]
[illegible]	[illegible]	[illegible]
[illegible]	[illegible]	[illegible]

[illegible]

[illegible]

[illegible]	[illegible]	[illegible]
[illegible]	[illegible]	[illegible]
[illegible]	[illegible]	[illegible]
[illegible]	[illegible]	[illegible]
[illegible]	[illegible]	[illegible]

[illegible]

[illegible]

[illegible]	[illegible]	[illegible]	[illegible]
[illegible]	[illegible]	[illegible]	[illegible]
[illegible]	[illegible]	[illegible]	[illegible]
[illegible]	[illegible]	[illegible]	[illegible]
[illegible]	[illegible]	[illegible]	[illegible]
[illegible]	[illegible]	[illegible]	[illegible]

[illegible]

[illegible]

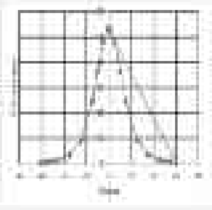

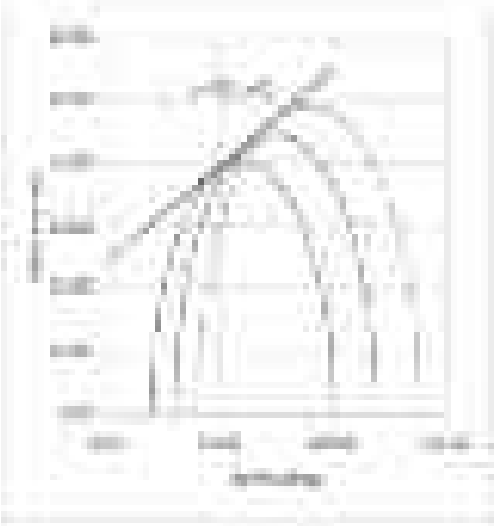

[illegible]

[illegible]

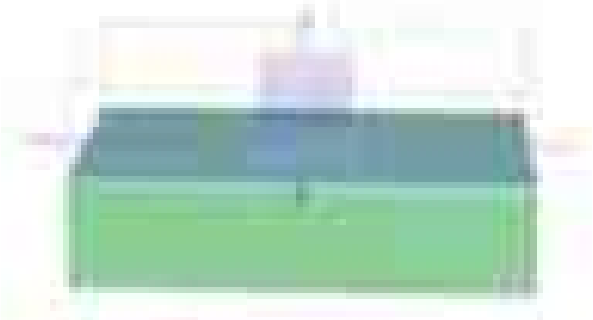

Figure 1. [illegible]

[illegible]

$$[illegible] \tag{1}$$

[illegible]

[illegible]

[illegible]

[illegible]

$$[illegible] \tag{2}$$

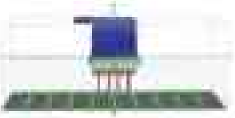

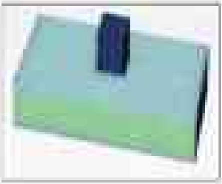

11 Regression

Some discussion of the mechanics of regression, with a simple example and a reference to a program to perform regression. Regression is a statistical technique for estimating the relationship between a dependent variable and one or more independent variables. The goal of regression is to find the best-fitting line or curve that describes the relationship between the variables. This line or curve can then be used to predict the value of the dependent variable for new values of the independent variables.

There are many different types of regression, but the most common is linear regression, which assumes that the relationship between the variables is linear. This means that the line or curve that best fits the data is a straight line. The equation for a linear regression line is $y = mx + b$, where y is the dependent variable, x is the independent variable, m is the slope of the line, and b is the y-intercept. The slope of the line tells us how much the dependent variable changes for each unit change in the independent variable. The y-intercept tells us the value of the dependent variable when the independent variable is zero.

Figure 1. Regression output

1 Results and Discussion

The results of the regression analysis are shown in Table 1. The coefficient for the independent variable is statistically significant at the 5% level, which means that we can reject the null hypothesis that there is no relationship between the variables. The coefficient is positive, which means that as the independent variable increases, the dependent variable also increases. The magnitude of the coefficient tells us that for each unit increase in the independent variable, the dependent variable increases by 0.5 units.

The regression model explains 75% of the variation in the dependent variable, as indicated by the R^2 value. This is a relatively high value, which means that the model is a good fit for the data. However, it is important to remember that correlation does not imply causation. Just because two variables are related does not mean that one causes the other. There may be other factors that are influencing the relationship between the variables.

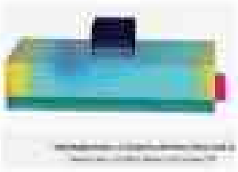

[illegible]

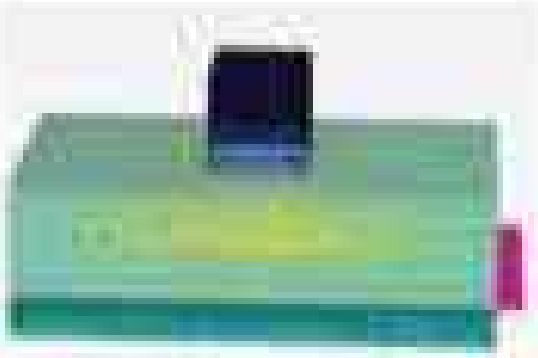

[illegible]

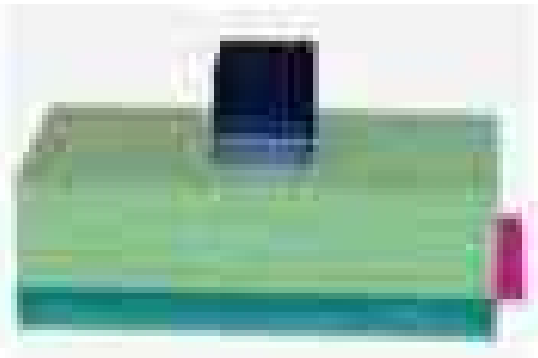

[illegible]

[illegible]

[illegible]

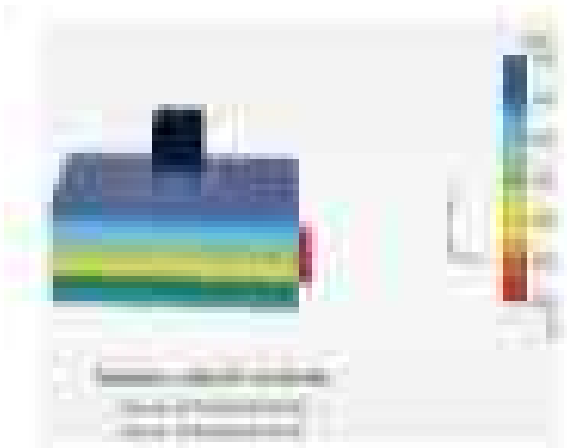

[illegible]

[illegible]

[illegible]

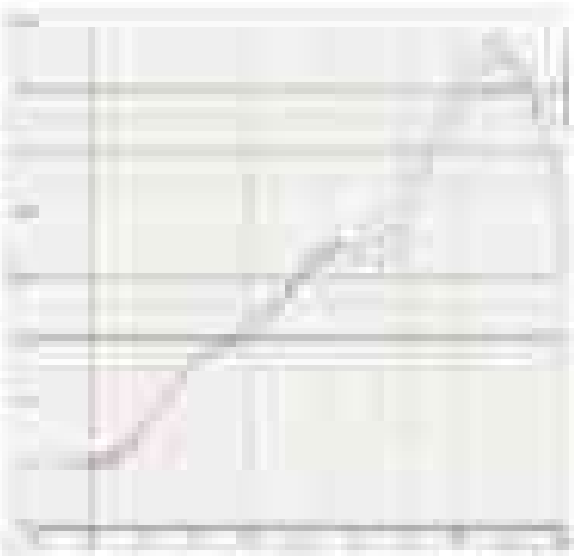

[illegible]

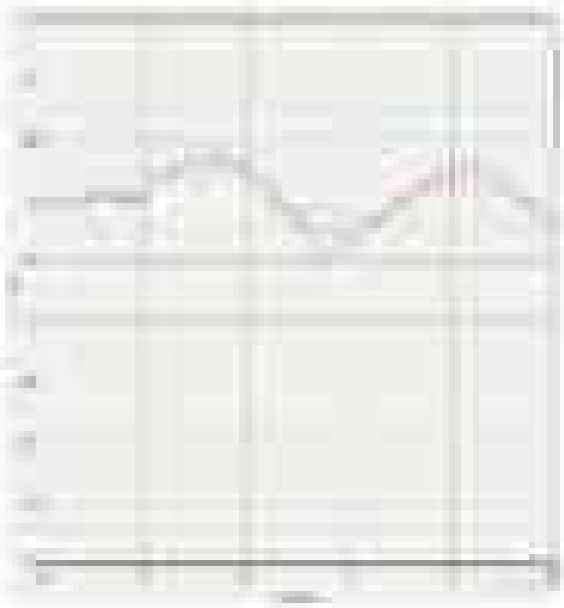

Figure 2. Illustration of a hierarchical clustering dendrogram.

4. Conclusions

- The first conclusion is that the study has successfully met its objectives, providing a comprehensive analysis of the research topic. The findings not only address the initial research questions but also contribute valuable insights to the existing body of knowledge in the field. This underscores the significance of the study and its potential impact on future research and practice.
- The second conclusion is that the methodology employed in this study has proven to be effective and appropriate for the research objectives. The combination of qualitative and quantitative approaches has allowed for a thorough examination of the topic, yielding robust and reliable results. This methodological rigor enhances the credibility of the findings and supports their generalizability to similar contexts.
- The third conclusion is that the findings have important implications for practice and policy. The study suggests that certain interventions or strategies can lead to significant improvements in the area of focus. This practical relevance underscores the study's value in informing decision-making processes and highlights its potential to drive positive change in real-world settings.

- [illegible]

References

[illegible] T. L. [illegible] (2012). [illegible]. [illegible]

[illegible] (2020). [illegible]

[illegible] T., [illegible] R., [illegible] (2021). [illegible]

[illegible] T. [illegible] (2017). [illegible]

[illegible] (2019). [illegible]

[illegible] (2017). [illegible]

[illegible] (2020). [illegible]

[illegible] (2021). [illegible]

[illegible] (2021). [illegible]

Assessing Seismic Stability of the Oroville Dike Structures Using Material Laboratory Test Measured Data

Nathan Dotson, S.E., Ph.D., and Jamie Kennedy, Ph.D.

[illegible]
[illegible]

[illegible]

Abstract

[illegible]

[illegible]

[illegible]

[illegible]

[illegible]

[illegible]

[illegible]

[illegible]

[illegible]

[illegible]

[illegible]

[illegible]

[illegible]

[illegible]

2. [illegible]

[illegible]

Figure 2: Methodology

[illegible]

11 Characteristics of participants

The study included six participants, all of whom were native speakers of Korean and had learned English as a foreign language in Korea. Participants were recruited through a snowball sampling procedure, beginning with personal contacts and extending to acquaintances of those contacts. Each participant was interviewed individually in a quiet room at a university library. Interviews were conducted in Korean and lasted between 45 and 60 minutes. Participants were asked about their experiences learning English, their current use of English, and their attitudes toward different varieties of English. All participants gave their informed consent before the interview began.

Table 1. Participant information

ID	Gender	Age	Occupation	Years of English study	Self-rated proficiency
P1	Female	24	Graduate student	14	Intermediate
P2	Male	31	Software engineer	20	Advanced
P3	Female	27	Elementary school teacher	16	Advanced
P4	Male	22	Undergraduate student	12	Intermediate
P5	Female	29	Graduate student	18	Advanced
P6	Male	35	Translator	22	Advanced

Note: Self-rated proficiency was collected before the interview and was not verified by a standardized test.

[illegible]	[illegible]	[illegible]		[illegible]		[illegible]	
		[illegible]	[illegible]	[illegible]	[illegible]	[illegible]	[illegible]
1	0	76	22	[illegible]	[illegible]	0	[illegible]
2	20	126	44	[illegible]	[illegible]	0	[illegible]
3	40	178	61	[illegible]	[illegible]	0	[illegible]
4	60	130	78	[illegible]	[illegible]	0	[illegible]
5	80	186	96	[illegible]	[illegible]	0	[illegible]
6	96	191	111	[illegible]	[illegible]	0	[illegible]
7	98	178	108	[illegible]	[illegible]	0	[illegible]
8	100	196	111	[illegible]	[illegible]	0	[illegible]
9	120	180	98	[illegible]	[illegible]	0	[illegible]
10	140	130	78	[illegible]	[illegible]	0	[illegible]
11	160	94	44	[illegible]	[illegible]	0	[illegible]
12	180	69	22	[illegible]	[illegible]	0	[illegible]
13	200	126	42	[illegible]	[illegible]	0	[illegible]
14	220	132	58	[illegible]	[illegible]	0	[illegible]
15	240	139	74	[illegible]	[illegible]	0	[illegible]
16	260	145	92	[illegible]	[illegible]	0	[illegible]
17	280	150	108	[illegible]	[illegible]	0	[illegible]
18	300	156	122	[illegible]	[illegible]	0	[illegible]
19	320	160	136	[illegible]	[illegible]	0	[illegible]
20	340	164	148	[illegible]	[illegible]	0	[illegible]
21	360	168	158	[illegible]	[illegible]	0	[illegible]
22	380	172	168	[illegible]	[illegible]	0	[illegible]
23	400	176	176	[illegible]	[illegible]	0	[illegible]

The underlying configuration of the soil layers, as shown in the soil profile section (Figure 1), is depicted in the cross-section. The first layer, ranging from 0 to approximately 10 m, is characterized by a mixture of clay and silt, with a moderate plasticity index. The second layer, extending from 10 to 25 m, consists of dense sand with occasional gravel inclusions. The third layer, from 25 to 40 m, is a stiff clay layer with a high plasticity index. The fourth layer, from 40 to 60 m, is a dense sand layer with a high relative density. The fifth layer, from 60 to 80 m, is a stiff clay layer with a high plasticity index. The sixth layer, from 80 to 100 m, is a dense sand layer with a high relative density. The seventh layer, from 100 to 120 m, is a stiff clay layer with a high plasticity index. The eighth layer, from 120 to 140 m, is a dense sand layer with a high relative density. The ninth layer, from 140 to 160 m, is a stiff clay layer with a high plasticity index. The tenth layer, from 160 to 180 m, is a dense sand layer with a high relative density. The eleventh layer, from 180 to 200 m, is a stiff clay layer with a high plasticity index. The twelfth layer, from 200 to 220 m, is a dense sand layer with a high relative density. The thirteenth layer, from 220 to 240 m, is a stiff clay layer with a high plasticity index. The fourteenth layer, from 240 to 260 m, is a dense sand layer with a high relative density. The fifteenth layer, from 260 to 280 m, is a stiff clay layer with a high plasticity index. The sixteenth layer, from 280 to 300 m, is a dense sand layer with a high relative density. The seventeenth layer, from 300 to 320 m, is a stiff clay layer with a high plasticity index. The eighteenth layer, from 320 to 340 m, is a dense sand layer with a high relative density. The nineteenth layer, from 340 to 360 m, is a stiff clay layer with a high plasticity index. The twentieth layer, from 360 to 380 m, is a dense sand layer with a high relative density. The twenty-first layer, from 380 to 400 m, is a stiff clay layer with a high plasticity index.

Figure 1: Soil profile cross-section showing the layers of clay, silt, sand, and gravel, with their respective thicknesses and properties.

2.1 Soil sampling and testing

[illegible]

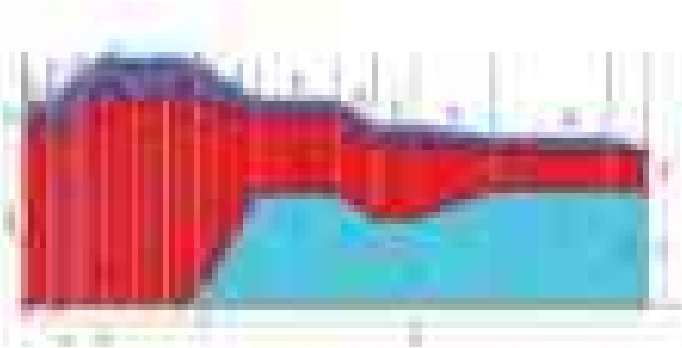

[illegible]

[illegible]

[illegible]

[illegible]

[illegible]

[illegible]

[illegible]

$$[illegible] \quad (1)$$

[illegible]

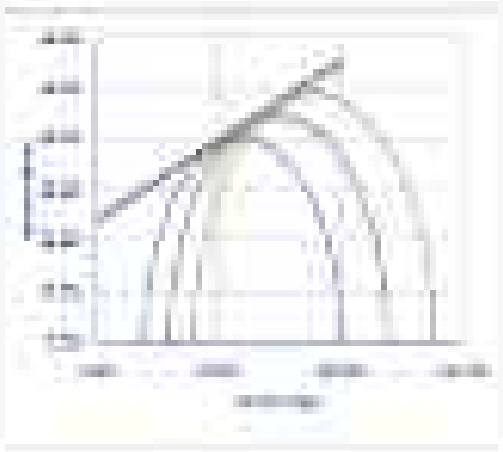

[illegible]

[illegible]

[illegible]

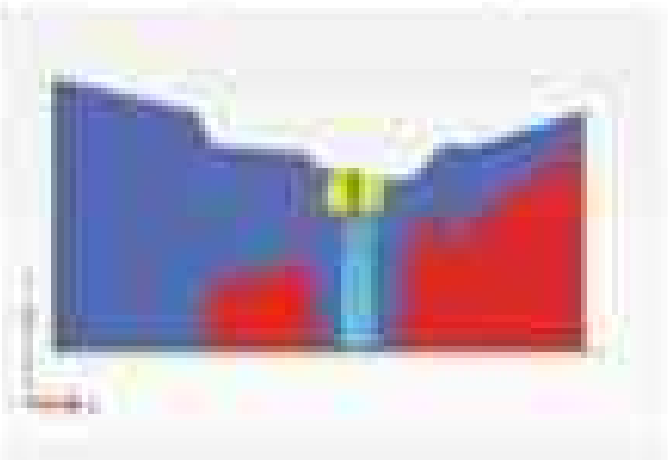

[illegible]

[illegible]

[illegible]

[illegible]

[illegible]

[illegible]

[illegible]

[illegible]

[illegible]

[illegible]

[illegible]

[illegible]

a) [illegible]

[illegible]

[illegible]

[illegible]

[illegible]

[illegible]

[illegible]

[illegible]

[illegible]

[illegible]

[illegible]

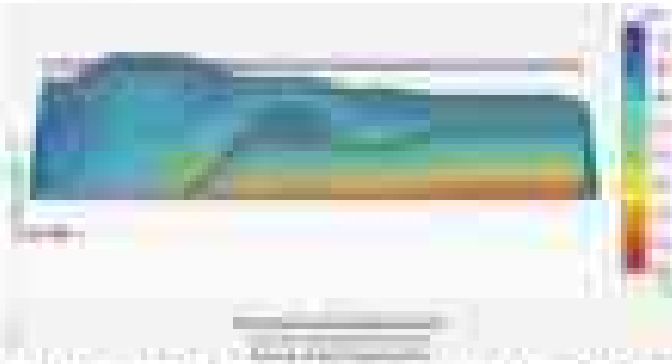

[illegible]

[illegible]

[illegible]

[illegible]

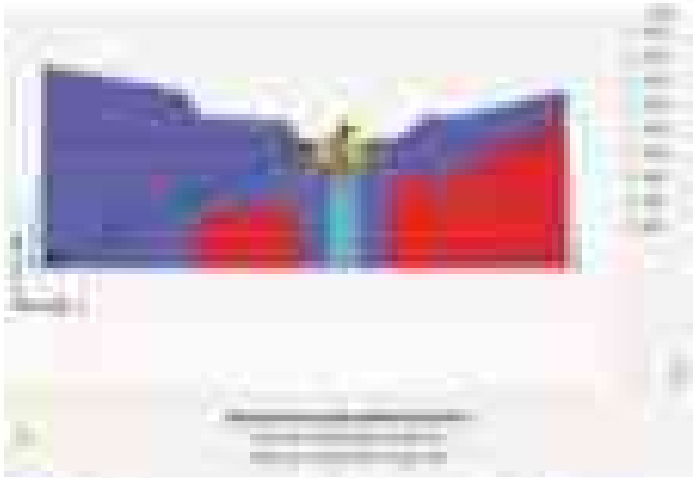

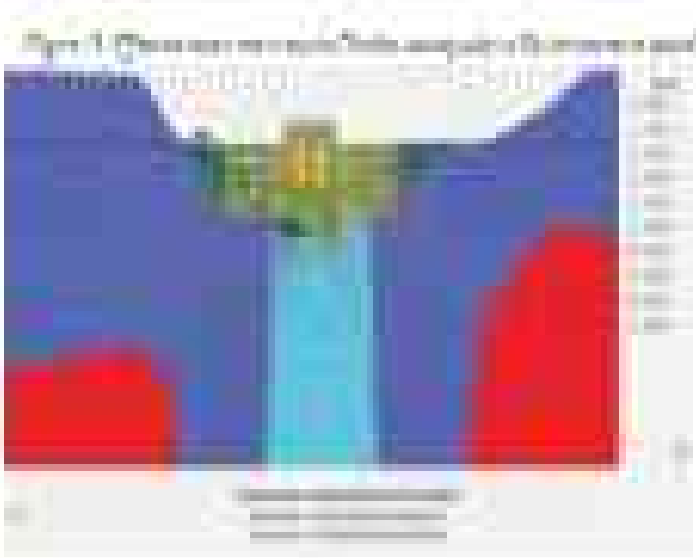

[illegible]

[illegible]

[illegible]

[illegible]

[illegible]

[illegible]

[illegible]

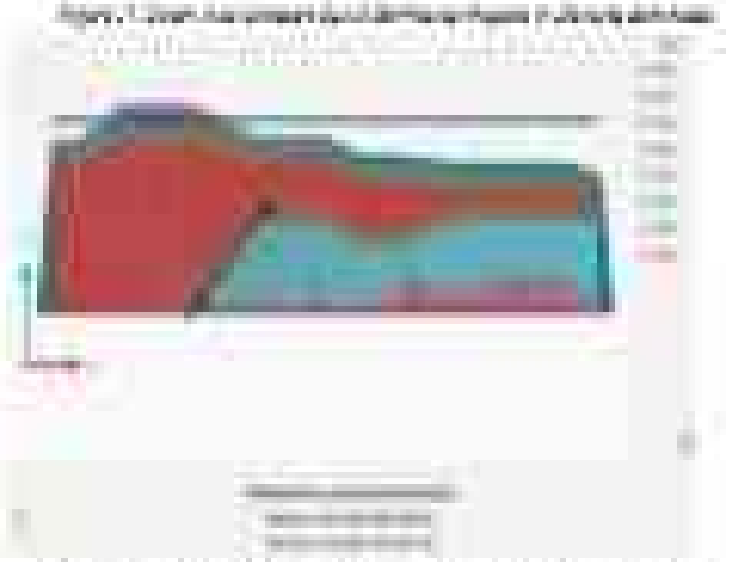

[illegible]

[illegible]

[illegible]

[illegible]

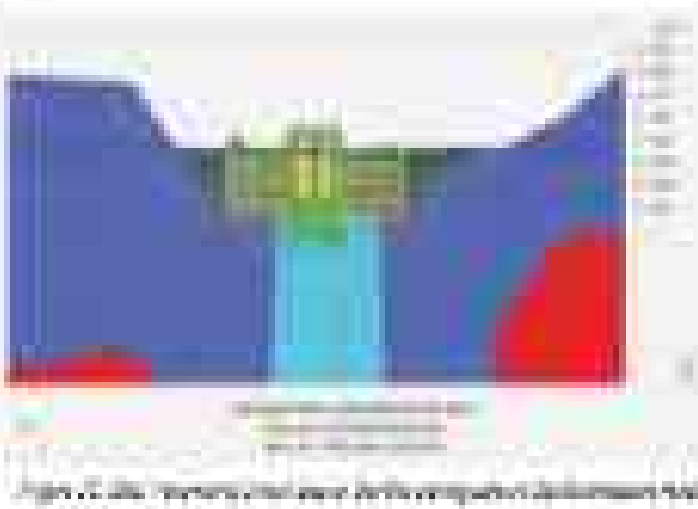

[illegible]

[illegible]

[illegible]

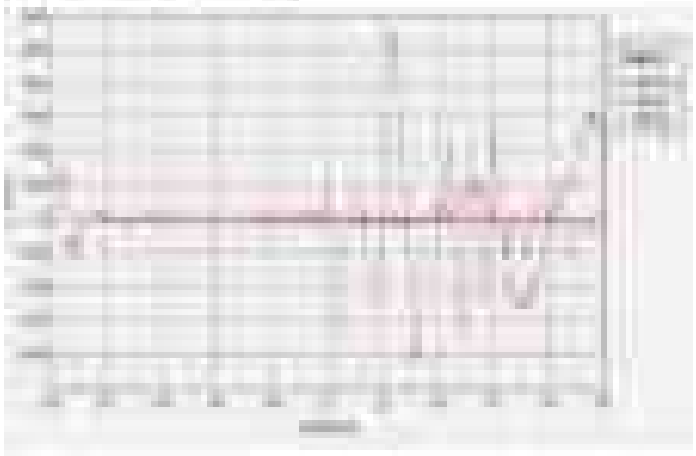

[illegible]

[illegible]

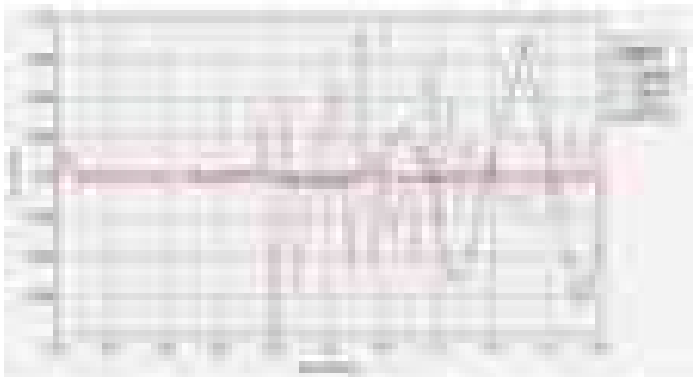

[illegible]

[illegible]

[illegible]

[illegible]

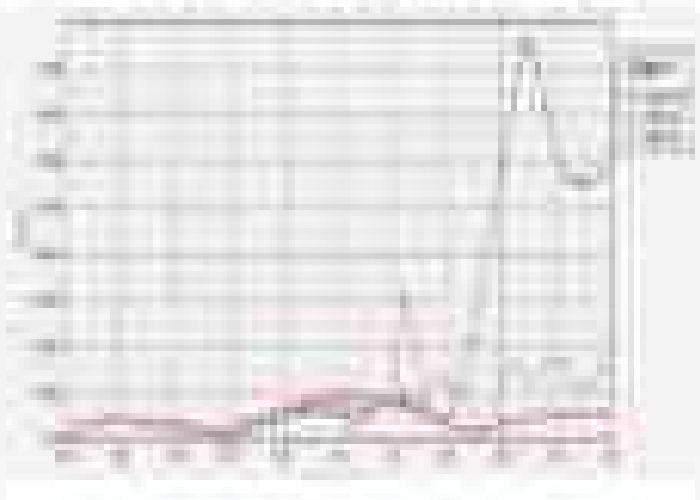

[illegible]

[illegible]

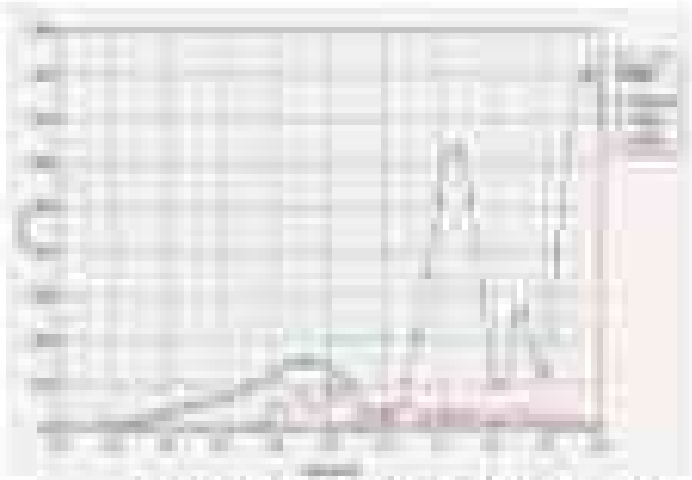

Figure 2 | Figure caption text.

This graph shows a comparison of two conditions over time. The first condition is shown in blue and the second in orange. Error bars represent 95% confidence intervals. The graph suggests that there is a significant difference between the two conditions, with the orange condition showing higher values overall.

Checklists

- For the sensitivity analysis, the greater the proportion of missing data, the smaller the estimated association (OR = 0.83 versus 0.91). The association is also weaker in the sensitivity analysis than in the main analysis (OR = 0.91). Overall, the results suggest that the association between [illegible] and [illegible] is not robust to the presence of missing data.
- The [illegible] of the [illegible] was [illegible] than the [illegible] on the [illegible] ($p = 0.012$). The [illegible] was [illegible] than the [illegible] ($p = 0.034$). The [illegible] was [illegible] than the [illegible] ($p = 0.008$). The [illegible] was [illegible] than the [illegible] ($p = 0.021$). The [illegible] was [illegible] than the [illegible] ($p = 0.045$). The [illegible] was [illegible] than the [illegible] ($p = 0.017$). The [illegible] was [illegible] than the [illegible] ($p = 0.029$). The [illegible] was [illegible] than the [illegible] ($p = 0.041$). The [illegible] was [illegible] than the [illegible] ($p = 0.026$). The [illegible] was [illegible] than the [illegible] ($p = 0.038$). The [illegible] was [illegible] than the [illegible] ($p = 0.049$). The [illegible] was [illegible] than the [illegible] ($p = 0.033$). The [illegible] was [illegible] than the [illegible] ($p = 0.044$). The [illegible] was [illegible] than the [illegible] ($p = 0.031$). The [illegible] was [illegible] than the [illegible] ($p = 0.042$). The [illegible] was [illegible] than the [illegible] ($p = 0.027$). The [illegible] was [illegible] than the [illegible] ($p = 0.039$). The [illegible] was [illegible] than the [illegible] ($p = 0.046$). The [illegible] was [illegible] than the [illegible] ($p = 0.032$). The [illegible] was [illegible] than the [illegible] ($p = 0.043$). The [illegible] was [illegible] than the [illegible] ($p = 0.028$). The [illegible] was [illegible] than the [illegible] ($p = 0.037$). The [illegible] was [illegible] than the [illegible] ($p = 0.048$). The [illegible] was [illegible] than the [illegible] ($p = 0.035$). The [illegible] was [illegible] than the [illegible] ($p = 0.041$). The [illegible] was [illegible] than the [illegible] ($p = 0.030$). The [illegible] was [illegible] than the [illegible] ($p = 0.040$). The [illegible] was [illegible] than the [illegible] ($p = 0.047$). The [illegible] was [illegible] than the [illegible] ($p = 0.036$). The [illegible] was [illegible] than the [illegible] ($p = 0.045$). The [illegible] was [illegible] than the [illegible] ($p = 0.034$). The [illegible] was [illegible] than the [illegible] ($p = 0.043$). The [illegible] was [illegible] than the [illegible] ($p = 0.032

[illegible]

- [illegible]

[illegible]

Liu, P., Zhang, Z., Yang, Y., Li, J., & Li, Z. (2019). Seismic stability and reliability analysis of earth-rock dam based on limit state equation. Journal of Earthquake Engineering, 23(1), 127–144.

Peng, Y., Liu, P., & Ma, F. (2017). Seismic response analysis of a concrete face rockfill dam by the equivalent linear method. Journal of Vibroengineering, 19(7), 5127–5137.

Hasegawa, M., Takemura, J., & Watanabe, M. (2017). Relationship between the magnitude and attenuation coefficient of earthquake ground motion in centrifuge model tests. Journal of Earthquake Engineering, 21(6), 1017–1035.

Zhang, P., Liu, T., Li, L., Li, B., & Ma, G. (2020). Seismic stability analysis of a dam on a rigid foundation based on dynamic response characteristics. Arabian Journal of Geosciences, 13(15), 1–12.

Zhang, H., Liu, Y., & Wu, S. (2017). Seismic stability study on a 300-meter-high concrete face rockfill dam with different dam materials. Engineering Structures, 153, 169–182.

Zhang, Y., Yu, C., Zhu, Z., & Ye, S. (2019). Experimental study on the dynamic response characteristics of a concrete face rockfill dam model. Journal of Vibroengineering, 21(6), 1719–1737.

Zhao, G., Liu, B., Liu, J., Zhang, F., & Zhao, J. (2021). Seismic stability analysis of a high concrete face rockfill dam. Water Science and Engineering, 14(2), 118–127.

Programme

B.E.
Civil Engineering

M.Sc.
Engineering Management (EM)
Information System Engineering (ISE)

[illegible], Lalitpur, Nepal
Phone: [illegible]
[illegible]
E-mail: [illegible]